Electrical characterization of as-grown, annealed and indium-doped Hg1-xZnxTe for x near 0.15

S. Rolland, A. Lasbley, A. Seyni, R. Granger, R. Triboulet

▶ **To cite this version:**

S. Rolland, A. Lasbley, A. Seyni, R. Granger, R. Triboulet. Electrical characterization of as-grown, annealed and indium-doped Hg1-xZnxTe for x near 0.15. Revue de Physique Appliquée, 1989, 24 (8), pp.795-802. 10.1051/rphysap:01989002408079500 . jpa-00246102

HAL Id: jpa-00246102
https://hal.science/jpa-00246102

Submitted on 4 Feb 2008

HAL is a multi-disciplinary open access archive for the deposit and dissemination of scientific research documents, whether they are published or not. The documents may come from teaching and research institutions in France or abroad, or from public or private research centers.

L'archive ouverte pluridisciplinaire **HAL**, est destinée au dépôt et à la diffusion de documents scientifiques de niveau recherche, publiés ou non, émanant des établissements d'enseignement et de recherche français ou étrangers, des laboratoires publics ou privés.

Classification
Physics Abstracts
72.20

Electrical characterization of as-grown, annealed and indium-doped $Hg_{1-x}Zn_xTe$ for x near 0.15

S. Rolland (1), A. Lasbley (1), A. Seyni (1), R. Granger (1) and R. Triboulet (2)

(1) I.N.S.A., Laboratoire de Physique des Solides, UA 040786 au C.N.R.S., F-35043 Rennes Cedex, France
(2) Laboratoire de Physique des Solides, LP 001332 au C.N.R.S., F-92195 Meudon Cedex, France

(*Reçu le 27 février 1989, accepté le 17 avril 1989*)

Résumé. — Les concentrations et mobilités des porteurs dans $Hg_{1-x}Zn_xTe$ pour x voisin de 0,15 sont données pour les matériaux bruts de tirage T.H.M. et après des recuits sous pression de mercure. Ces concentrations et mobilités sont voisines de celles trouvées dans $Hg_{1-x}Cd_xTe$ de même largeur de bande interdite ($x = 0{,}22$). Cependant le coefficient de diffusion du mercure est bien plus faible, ce qui rend plus difficile l'obtention d'échantillons homogènes de type n par recuit stœchiométrique à basse température, mais traduit une meilleure stabilité du matériau. L'indium est donneur mais a aussi un faible coefficient de diffusion ; de plus ce dopage diminue fortement la mobilité des électrons. Il est possible de décrire raisonnablement la mobilité des porteurs et la concentration intrinsèque en utilisant un modèle de Kane pour la bande de conduction. Ce modèle conduit à une estimation de la masse effective des trous lourds voisine de $0{,}6\ m_0$.

Abstract. — Concentration and mobility of carriers in $Hg_{1-x}Zn_xTe$ for x near 0.15 are presented for as grown T.H.M. material and after annealings under mercury pressure. These concentrations and mobilities are near those found in $Hg_{1-x}Cd_xTe$ for a same band gap ($x = 0.22$). However the mercury diffusion coefficient is lower, this involves difficulty to obtain homogeneous n-type samples through low temperature stoichiometric annealing but reveales a better stability of the material. Indium is a donor dopant but with also a low diffusion coefficient ; moreover this doping strongly decreases the electron mobility. Carrier mobility and intrinsic concentration can be well described with a Kane model for the conduction band. This model leads to an estimation for the heavy hole effective mass of $0.6\ m_0$.

1. Introduction.

Since a few years, $Hg_{1-x}Zn_xTe$ (MZT) appears as an alternative material to $Hg_{1-x}Cd_xTe$ (MCT) due to the lack of stability in this last semiconductor, especially for Hg-rich solid solutions used in detectors in the 10 μm wavelength range. First theoretical [1, 2] and experimental [3-6] studies revealed a better stability and lower composition fluctuations in MZT materials. Infrared detectors in the 8-12 μm range have been made using the process technology already used in MCT [7, 8]. In spite of non optimized conditions, these detectors have got performances comparable to MCT ones. Moreover devices lifetime is improved under high temperature tests, confirming a better stability of MZT [8].

A good knowledge of conditions giving definited samples (type, concentration, mobility) is now necessary for device processing optimization.

In this paper we present first detailed analysis of treatments for carrier concentration adjustements either by equilibrium of native defects or by doping with some impurities.

In section 2 we describe experimental processes in order to obtain homogeneous samples with well defined type and carrier concentrations. This is obtained by adjustment of sample temperature and mercury partial vapor pressure. Experimental techniques for electrical measurements are also presented. In section 3 experimental results and the method used to deduce carrier concentrations and mobilities of p-type samples in the mixed conduction range are reported. In section 4, p to n type conversion which is essential for devices applications is presented. This is obtained from stoechiometric annealing at low temperature and from indium doping through vapor transfert. In section 5 mobility and carrier concentrations are discussed in the framework of the Kane model.

Article published online by EDP Sciences and available at http://dx.doi.org/10.1051/rphysap:01989002408079500

2. Experimental processes.

2.1 ANNEALING TREATMENTS. — Ingots with composition x near 0.15 are grown by the Travelling Heater Method (THM) [3, 6, 9]. Circular slices of 15 mm diameter and 1 mm thickness are then cut with a wire saw. Prior to anneals or electrical measurements samples are cleaned in trichlorethylene, rinsed and chemically etched in methanol-Br (2 %) at room temperature, then rinsed a new time [5].

Annealing treatments are performed in a two temperatures furnace. Samples are placed in cleaned quartz ampoules evacuated at 10^{-5} Pa of argon at temperature T_1, and mercury at temperature T_2 lower than T_1. T_2 controls the partial pressure of mercury. High temperature annealings correspond to $T_1 = 400$ °C ($T_2 = 380$ °C) and $T_1 = 500$ °C ($T_2 = 460$ °C or 350 °C). After each anneal, samples are rapidly air or water quenched. In these conditions, as shown in the next part, samples are p-type. Annealing times were verified to be sufficient to obtain homogeneous samples. Such anneals allow adjustement of carrier concentration but also eliminate tellurium precipitates occuring during the THM growth with tellurium solvent [2].

Low temperature annealings were made at $T_1 = 260$ °C and $T_2 = 240$ °C as usual in MCT in order to obtain n-type samples. The kinetics of the p to n-type conversion is very sensitive to anterior annealings.

Indium vapor phase doping has been also performed at $T_1 = 500$ °C putting a In_yHg_{1-y} alloy with adjusted y in place of pure mercury at $T_2 = 460$ °C.

2.2 CHARACTERIZATION. — Electric contacts are obtained by an electrolytic deposition of Ni, followed by an Au one. 50 μm diameter gold wires are then soldered using an In-Pb-Bi alloy giving low thermovoltage and low temperature fusion point. These contacts remain ohmic down to 4.2 K, both on p or n type samples.

Electrical measurements are made in the Van der Pauw configuration. First they are monitored in a conventional magnet giving magnetic fields up to 1 Tesla, in a cryostat allowing 77 K-300 K temperature variations, with a good stability. Good samples are then choosen and new measurements are made between 4 K and 300 K using a superconducting magnet where the induction reaches 4 Teslas.

An automatic monitoring system followed by a microcomputer treatment allows data acquisition for each B and T value. Calculations give resistivity (ρ) and Hall coefficient (R_H) variations with temperature and magnetic field.

3. Experimental results on p-type samples.

3.1 AS-GROWN SAMPLES. — The resistivity value remains approximatly constant in the 100 K-300 K range (Fig. 1) about 10^{-3} Ω.m ; a sharp increase appears at lower temperatures ; ρ goes up to 10^{-1} Ω.m at 4.2 K. To explain these results it is necessary to study carrier concentrations and mobilities variations with temperature.

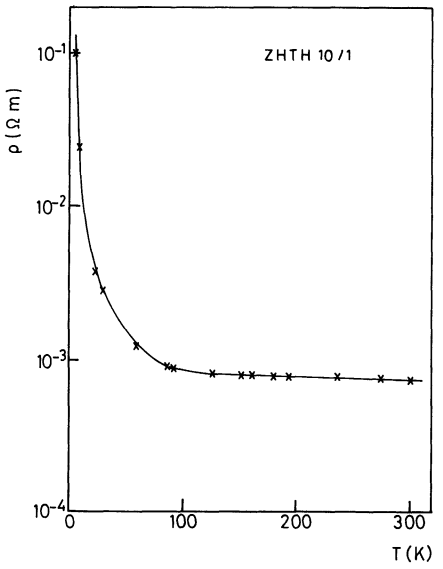

Fig. 1. — Temperature dependence of electrical resistivity on an as-grown sample.

Typical R_H variations with temperature are shown in figure 2 for magnetic field $B = 0.1$ T and 1 T. The change of R_H sign with temperature depends on the magnetic field. This indicates a mixed conduction, as expected in small gap semiconductors ($x = 0.15$)

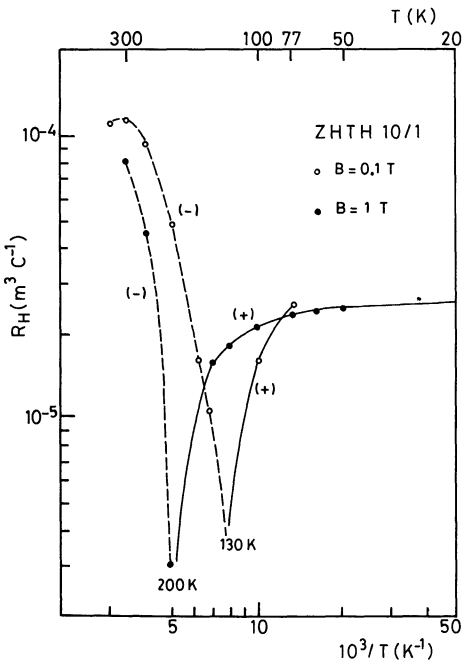

Fig. 2. — Temperature dependence of Hall coefficient at two magnetic fields : (+) means R_H positive ; (−) R_H negative.

where the intrinsic concentration at 300 K is in the range of 10^{16} cm^{-3}. The mixed range depends of course on the hole concentration p. Given a p value, it appears a plateau on the R_H curves *versus* T at low temperature. This plateau allows to determine the extrinsic hole concentration p_0 as shown in figure 3 from the usual formula $R_H = \frac{1}{p_0 e}$ assuming a diffusion factor equal to 1. The increase of R_H at lower temperatures is attributed to the ionization of an acceptor whose characterization is not studied here.

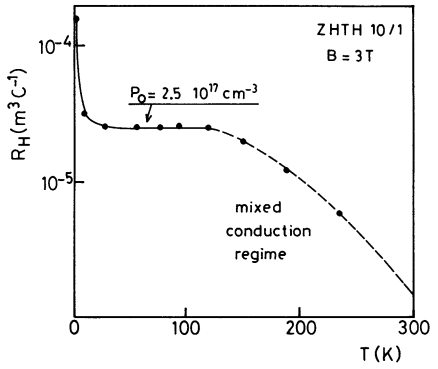

Fig. 3. — p_0 determination from curve $R_H(T)$ at $B = 3$ T ; in doted line mixed conduction regime.

When temperature increases, intrinsic electrons appear and calculations in the mixed conduction range are done using the assumptions of spherical energy bands, parabolicity and energy independent relaxation time [10]. With these assumptions :

$$R_H = \frac{1}{e} \frac{p\mu_p^2 - n\mu_n^2 + \mu_p^2 \mu_n^2 B^2 (p-n)}{(p\mu_p + n\mu_n)^2 + \mu_p^2 \mu_n^2 B^2 (p-n)^2}$$

p and n are respectively the hole and electron concentrations, μ_p and μ_n their mobilities. Moreover $\sigma = e(p\mu_p + n\mu_n)$ and $p_0 = p - n$ corresponding to charge conservation. Resolution of such equations needs σ, p_0 and two R_H values obtained at two different magnetic fields. Solving the four equations using Newton method, gives p, μ_p, n, μ_n at each temperature in the mixed conduction range. The intrinsic electron concentration n_i is then deduced by $n_i^2 = n \cdot p$. Assuming n_i proportional to $T^{3/2}\, e^{-E_g/2kT}$, where E_g is the band gap energy at $T = 0$ K, a plot of $n_i/T^{3/2}$ as a function of $\frac{1}{T}$ (Fig. 4) gives the E_g value from the linear part of the curve. The linear gap variation with temperature assumed here has been verified down to 50 K [6]. The E_g values so deduced are compared with those obtained by optical measurements [6]. From the E_g value, we obtain the x composition of the samples. A very fine agreement is found between

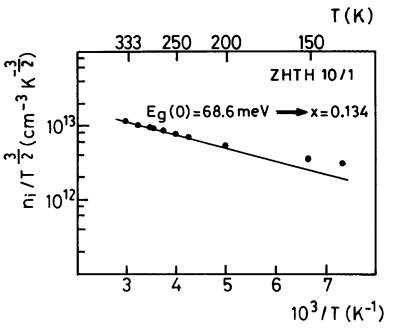

Fig. 4. — $n_i/T^{-3/2}$ *versus* 1 000/T.

the x determination through n_i and $\langle x \rangle$ measured by microprobe analysis [11] (Tab. I) in view of composition inhomogeneity.

Table I. — *Characteristics of as grown samples : p_0 extrinsic concentration ; n_i intrinsic concentration at* 300 K ; E_g(0 K) *energy gap ; x calculated composition (Cf. Sect.* 3.1) ; $\langle x \rangle$ *mean value obtained from microprobe analysis ; x_{mini} and x_{max}, extrema of these measurements.*

Sample	P_o (cm^{-3})	n_i (cm^{-3})	Eg(o) (meV)	x calculated	$\langle x \rangle$	x mini	x max
ZHTH 10/1	2.5 10^{17}	2.93 10^{16}	68	0.132	0.137	0.126	0.146
ZHTH 14/1	5.1 10^{17}	2.57 10^{16}	117	0.145	0.157	0.145	0.169
ZHTH 27/11	21 10^{17}	5.27 10^{16}	47	0.126	0.124	0.112	0.139
ZHTM 11/2	5.6 10^{17}	2.04 10^{16}	111	0.150	0.160	0.151	0.170
ZHTM 13/2	5.2 10^{17}	1.63 10^{16}	52	0.128	0.159	0.146	0.176

However carrier concentration evaluations in the mixed regime are limited in the temperature range 200 K-300 K. Below 200 K, the intrinsic concentration is too small and the method gives significant errors (See Fig. 4).

At low temperatures, as shown in figure 3, R_H increases rapidly. The hole concentration decreases and μ_p remains approximatly constant [5], this explains the increase of resistivity at 4.2 K.

In table II, results obtained on as-grown samples issued from two ingots ZHTH and ZHTM are shown. In the first ZHTH ingot, p_0 increases from the beginning of the ingot (ZHTH 8/1) to the end with a stronger variation at the end of the ingot (ZHTH 27/3). This p_0 concentration is correlated to the longitudinal x composition [3]. The hole concentration appears more homogeneous in the second ingot where $p_0 \simeq 6 \times 10^{17}$ cm^{-3}.

3.2 ANNEALED SAMPLES. — First annealings were made with $T_1 = 400$ °C and $T_2 = 380$ °C during 114 h. Results of concentrations and mobilities at 77 K and 300 K are shown in table III. An equilibrium state is reached with $p_0 \simeq 1.2 \times 10^{17}$ cm^{-3}. New

Table II. — *Electronic properties of as-grown samples : 2 A ZHTH ingot, 2 B ZHTM ingot.*

Sample	P_o (10^{17} cm^{-3})	μ_p (cm^2/V.s)		μ_n(cm^2/V.s)
		290 K	77 K	(290 K)
ZHTH 8/1	1.8	268	308	8160
ZHTH 10/1	2.5	262	210	7400
ZHTH 14/1	5.1	208	205	6400
ZHTH 23/13	26	102	129	11440
ZHTH 23/33	26	112	140	11920
ZHTH 27/11	21	108	127	9880

Sample	P_o (10^{17} cm^{-3})	μ_p (cm^2/V s)		μ_n(cm^2/V s)
		290 K	77 K	(290K)
ZHTM 11/2	5.6	136	204	7500
ZHTM 12/2	6.7	121	180	6316
ZHTM 13/2	5.2	155	200	10548
ZHTM 14/2	6.7	—	160	—
ZHTM 15/1	5.0	161	231	7200

Table III. — *Electronic properties after annealing with T_1 = 400 °C, T_2 = 380 °C.*

Sample	Annealing time(hours)	P_o (10^{17} cm^{-3})	μ_p(cm^2/V.s)		μ_n(cm^2/V.s)
			290 K	77 K	(290 K)
ZHTH 8/5	114	0.35	505	316	11820
ZHTH 14/5	114	1.4	154	162	8990
ZHTH 27/3	114	1.25	395	417	10800
ZHTM 13/3	237	1.2	330	231	11038
ZHTM 10/1	237	1.16	240	373	8709

annealings in order to control p_0 with Hg pressure are performed changing T_2. T_1 = 500 °C has been next choosen to get a higher diffusion rate of the species and then, shorter annealing times to equilibrate samples.

According to Vydyanath results [12] in MCT case (with $x = 0.2$ corresponding to the same band gap as MZT with $x = 0.15$), p_0 would change with a P_{Hg}^{-1} law, P_{Hg} being the mercury partial pressure. Acceptor centers are doubly ionized mercury vacancies. At high mercury pressure : T_2 = 460 °C, the P_{Hg} high value limit the vacancies concentration and then p_0. When T_2 is smaller (for example 350 °C) this number will increase and we can expect higher p_0.

In table IV and V results are shown for these two T_2 temperatures. For T_2 = 460 °C, this corresponds to a mercury vapor pressure of 3.5 atmospheres and the resulting p_0 is 5×10^{17} cm^{-3}. For T_2 = 350 °C, P_{Hg} = 1 atmosphere and $p_0 = 1.9 \times 10^{18}$ cm^{-3}. These first results of p_0 *versus* P_{Hg} for MZT are

Table IV. — *Electronic properties after annealing with T_1 = 500 °C, T_2 = 460 °C.*

Sample	Annealing time(hours)	P_o (10^{17} cm^{-3})	μ_p(cm^2/V.s)		μ_n(cm^2/V.s)
			290 K	77 K	(290 K)
ZHTH 10/23	384	3.6	224	246	8365
ZHTM 13/4	96*	5.2	180	186	7094
ZHTM 14/4	96	6	150	169	7190
ZHTM 14/12	96	5.6	145	159	7158
ZHTM 14/3	96*	5.18	130	171	8389

* Previously annealed at 400/380°C during 237h

Table V. — *Electronic properties after annealing with T_1 = 500 °C, T_2 = 350 °C.*

Sample	Annealing time(hours)	P_o (10^{17} cm^{-3})	μ_p(cm^2/V.s)		μ_n(cm^2/V.s)
			290 K	77 K	(290 K)
ZHTH 8/5	136	19	104	110	8250
ZHTM 15/4	111	11	130	121	6140

reported in figure 5 with those of Vydyanath [12] for comparison. The P_{Hg}^{-1} law appears verified like in MCT so the same defect model may be applied. Nevertheless the p_0 values are higher in MZT. A detailed investigation with different T_1 and T_2 temperatures is necessary and currently performed in order to obtain the mass action law constants.

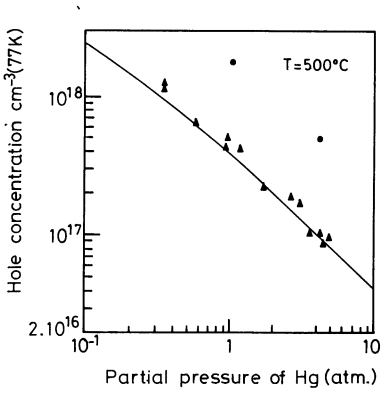

Fig. 5. — p_0 variations with mercury partial pressure : (▲) : $Hg_{1-x}Cd_xTe$ case [12] ; (●) : our results.

4. p to n-type change.

4.1 STŒCHIOMETRIC ANNEALING. — Considering that concentration p_0 decreases when the annealing temperature T_1 decreases, annealings were made with T_1 = 260 °C and T_2 = 240 °C. In the MCT case, this gives n-type homogeneous samples. But on MZT as-grown samples, only an n-type surface layer appears. Its thickness, as given by thermoelectric probing, follows a $\sqrt{t}$ law, t being the annealing time (Fig. 6). From these measurements, a diffusion

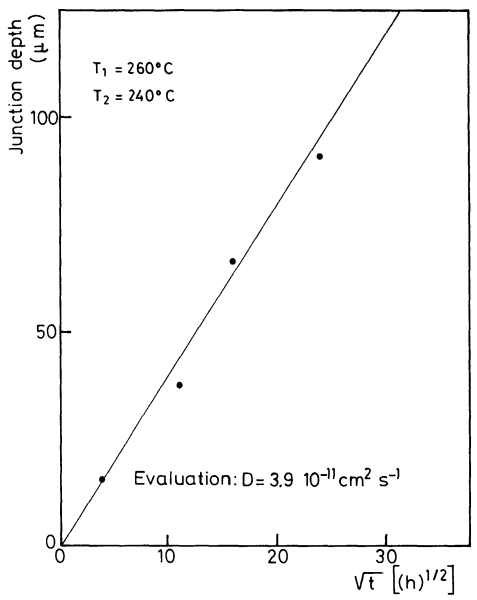

Fig. 6. — *n-p* front depth *versus* the root square of annealing time for $T_1 = 260$ °C and $T_2 = 240$ °C.

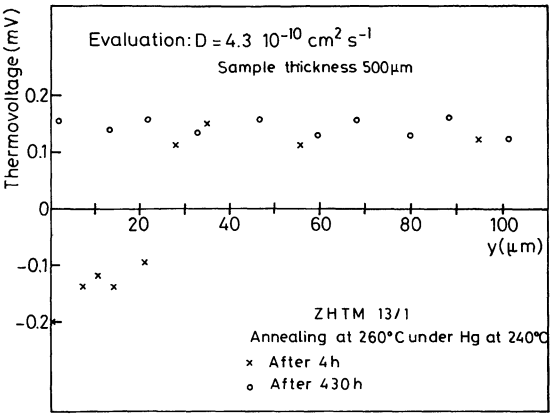

Fig. 7. — Thermoelectric signal *versus* position, after annealing at 260 °C-240 °C : (×) after 4 h ; (○) after 430 h. The sample was previously annealed at 400 °C-380 °C during 96 h.

coefficient for p to n-type change has been estimated to be $D = 3.9 \times 10^{-11}$ cm^2.s^{-1}. With this value of D it is necessary to anneal during about 200 days a one mm thick sample to have an n homogeneous sample.

At the present time, a complete understanding of p to n-type conversion mechanism is not available in MCT. It is commonly assumed that annealing with mercury overpressure fills mercury vacancies which are acceptors and the conversion to n-type results from residual donor impurities ; but donors due to interstitial mercury cannot be ruled out [13]. The situation is also complicated by the presence of excess tellurium, likely precipitates, and unknown residual acceptor impurities. The same problems are of course encountered in MZT. In order to test the influence of Tellurium precipitates in MZT, we have performed a preliminary long time annealing with $T_1 = 400$ °C and $T_2 = 380$ °C, followed by a low temperature annealing with $T_1 = 260$ °C, $T_2 = 240$ °C during 4 hours. The thickness deduced from thermoelectric probing was about 30 μm (Fig. 7) giving a diffusion coefficient of 4.3×10^{-10} cm^2.s^{-1}, which is about ten times higher than the first given value. These results are near those of Harman in MCT [13] and can be explained by a dissolution of tellurium precipitates after a high temperature annealing. Nevertheless the diffusion coefficient remains smaller in MZT.

Subsequent low temperature annealing has been then performed during the very long time of 430 hours in order to obtain an n-type homogeneous sample. The sample was homogeneous but p-type, as shown in figure 7. Such results have been obtained in MCT [14] and the explanation remains the same. Excess tellurium in the material dissolves a high concentration of acceptor impurities. As the annealed n part progresses from the surface of the sample, this excess of tellerium disappears and releases its solved impurities. These ones fast diffuse through the matrix under their induced concentration gradient toward the core of the sample where they are gettered. For a long enough annealing time all tellurium in excess is removed over all the sample leading to a uniform redistribution of these impurities.

The residual acceptor concentration appears to be higher in the samples than the donor one. The acceptors come probably from the starting Zn which is not of electronic grade. Refining processes are currently carried out to overcome this difficulty which is not dramatic for device elaboration when keeping a p-type core [15] but critical for material characterization.

Concentration n and mobility of electrons in the n layer are deduced from electrical measurements and its thickness using the model of Petritz [16] in a two-

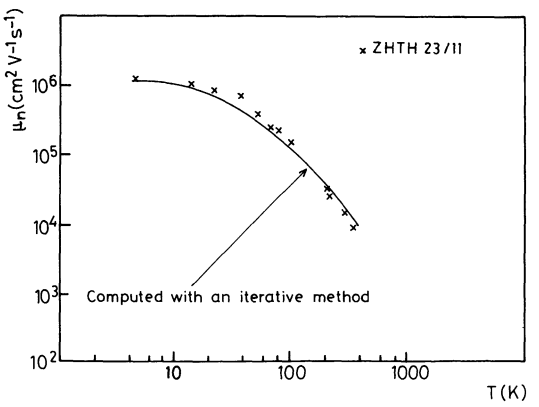

Fig. 8. — Temperature variation of electron mobility : (×) experimental results ; (–) calculated curve by an iterative method.

layer model. n is about 10^{16} cm^{-3} and mobility variations with temperature appear in figure 8. Theoretical calculations describing these variations are presented in the part 5.

4.2 VAPOR PHASE INDIUM DOPED SAMPLES. — Doping by In is done through vapor phase. Annealings with $T_1 = 500$ °C and $T_2 = 460$ °C are performed during 104 hours, with an Hg-In (50/50) alloy at temperature T_2. By thermoelectric probing at room temperature, and n-type layer of 70 μm thickness is found (Fig. 9). The value of the estimated diffusion coefficient is 8.3×10^{-11} cm^{-2}.s^{-1} which is ten times the corresponding value found in MCT at 500 °C after In implantation [17].

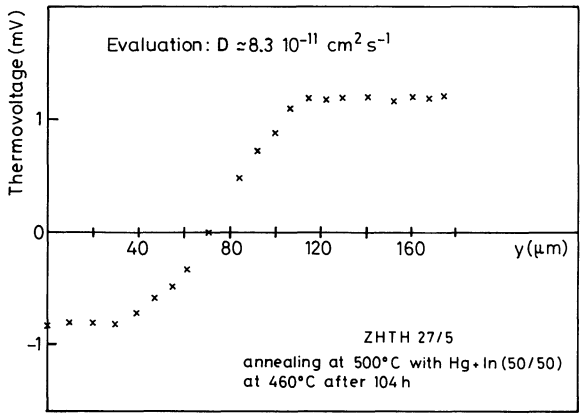

Fig. 9. — Thermoelectric signal *versus* position, on indium doped sample.

For these samples R_H is constant with magnetic field ; its variations with T are presented in figure 10, the corresponding electron concentration is 1.85×10^{18} cm^{-3}. The electron mobility is low (Fig. 11) reaching only 4×10^3 cm^2/V.s at 4.2 K instead of the 10^6 cm^2/V.s value found after a stœechiometric annealing. As shown by Vydyanath [18] in MCT for $x = 0.2$, only a few percent of indium gives donor

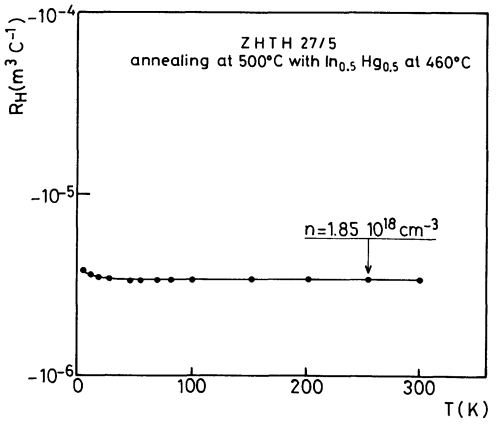

Fig. 10. — R_H variation with T on indium doped sample.

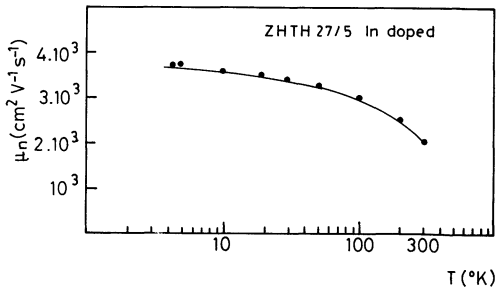

Fig. 11. — Electron mobility *versus* temperature on indium doped sample.

centers, the remainder, which remains neutral, limits the electron mobility due to supplementary scattering interaction (neutral impurity or core scattering).

5. Discussion.

5.1 ELECTRON MOBILITY. — Electron mobility results deduced from the mixed conduction range described in section 2 can be obtained only in the temperature range 200-300 K. Their values vary between 12 000 cm^2/V.s and 6 000 cm^2/V.s at 300 K and do not appear correlated with hole concentration p_0.

From layered samples, n-type mobilities were obtained in the range 4.2 K-300 K (see Fig. 8). Electron mobility has been calculated using an iterative method to solve the Boltzman transport equation in the two band Kane model [19, 20, 5]. A great number of the necessary parameters are presently unknown. A linear interpolation of their values for the binaries HgTe and ZnTe is tentatively done [5].

Moreover, the **k·p** matrix element P_{cv} and the spin orbit coupling Δ values have been taken the same as for MCT [21, 22]. With these assumptions, calculated results (Fig. 8) agree with experimental ones, if we consider optical and acoustical phonon scattering, ionized impurity scattering, disordered alloy scattering with a core radius of $r_0 = 2$ Å and a scattering center concentration of 2×10^{21} cm^{-3} [5]. Nevertheless, in the lack of knowledge of band edge effective mass for electrons, it is not usefull to go deeper in the scattering mechanisms any longer.

For n-type indium doped samples, we find only mobilities up to 4 000 cm^2/V.s. This agrees with results in MCT of similar n-type concentrations [17, 18] : only low fraction of indium in the matrix would give a donor state.

5.2 HOLE MOBILITY. — Hole mobilities *versus* temperature are show in figure 12 between 77 K and 300 K for different p_0 values which reveals a decrease of mobility when p_0 increases. More significantly figure 13 and figure 14 show the hole mobilities at

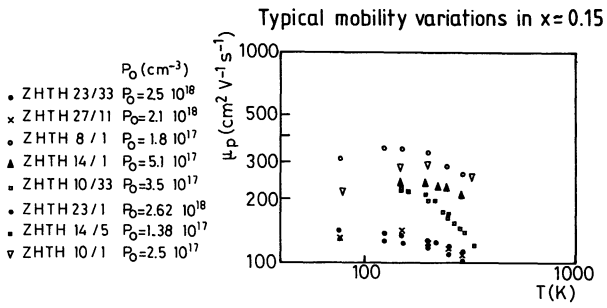

Fig. 12. — Temperature dependence of hole mobility for several samples.

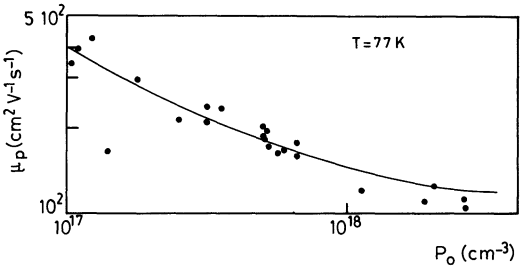

Fig. 13. — Hole mobility variations with p_0 at 77 K. Experimental results on MZT, solid curve : results on MCT [12].

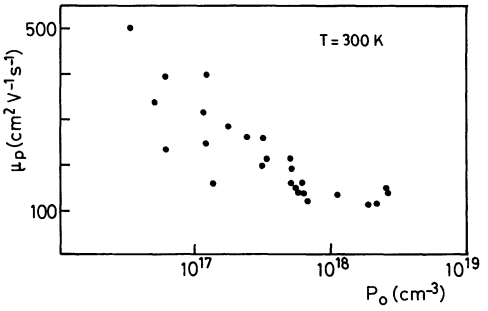

Fig. 14. — Hole mobility variations with p_0 at 300 K.

77 K and 300 K. At 77 K, the behaviour is very similar to MCT one, where Vydyanath deduced it is due to doubly ionized acceptors [18]. Although it is presumably the same in MZT, we have not yet got sufficient informations to conclude ; specially, doping by acceptor impurities like copper is necessary. At this stage of knowledge it is more difficult to evaluate the hole mobility since too much band parameters are necessary.

At 300 K, the strong decrease of mobility for higher p_0 cannot be explained by usual scattering mechanisms. It would be necessary to introduce others scattering processes to describe the actual values.

5.3 INTRINSIC CARRIER CONCENTRATION AT 300 K. — n_i is deduced from p and n concentrations values ($n \cdot p = n_i^2$). These 300 K values *versus* the sample mean composition $\langle x \rangle$ are presented in figure 15 ; $\langle x \rangle$ measurements are taken on samples used for electrical measurements or neighbour samples by electronic microprobing [11]. Examples of $\langle x \rangle$ and n_i values appear in table I.

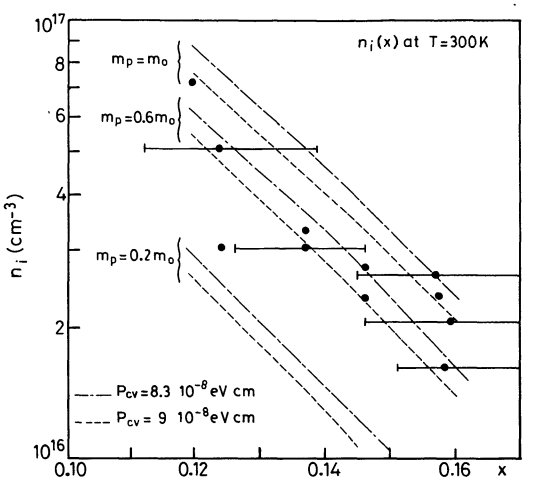

Fig. 15. — Intrinsic concentration n_i *versus* x composition : (•) : experimental determination from section 3.1. The bars indicate incertitudes on x composition as seen in table I. Curves are calculated using Kane model with two values of matrix element P_{cv} and three values of hole effective mass.

In order to calculate n_i, the following step is used : x and T being choosen, $E_g(x, T)$ is obtained from [6]. A test value for the electron concentration is taken ; then the Fermi energy E_F is deduced with a non parabolic conduction band using the Kane model [23]. The hole concentration corresponding to this E_F value is calculated with the Fermi Dirac statistics and a parabolic heavy hole band. The heavy hole effective mass m_p is taken as a parameter and the light hole valence band is omitted. An iterative process gives the n value corresponding to $n = p = n_i$. Calculations were performed at 300 K for three m_p values : $m_p = 0.2\ m_0$, $m_p = 0.6\ m_0$ and m_0. The Kane matrix element P_{cv} is almost constant in II-VI compounds [21], [24-30]. The extrem values reported $P_{cv} = 9 \times 10^{-8}$ eV.cm and $P_{cv} = 8.3 \times 10^{-8}$ eV.cm have been used for each m_p value. The curves are drawn in figure 15 and compared with data deduced from experiments. A good fit is obtained for $m_p = 0.6\ m_0$. The incertitudes on experimental x values do not allow a more precise parameters determination.

6. Conclusion.

First reliable results on carrier concentration and mobility of $Hg_{1-x}Zn_xTe$ for $x = 0.15$ after annealing under mercury pressure are presented. Samples remain p-type for annealing temperature above

300 °C : their concentration depends on mercury pressure. At lower temperature ($T = 260$ °C) it is possible to convert p-type to n-type by annealing under mercury pressure (stoichiometric annealing) which decreases mercury vacancies.

The kinetics of this conversion is low compared to the corresponding one in $Hg_{1-x}Cd_xTe$ for $x \simeq 0.2$ revealing a better stability of this material despite its higher mercury composition.

This kinetics is also controlled by the excess of tellurium present in samples. Moreover, the residual acceptor concentration appears higher than the donor one. This situation does not allow to obtain at the present time thick n-type homogeneous samples. n-type doping by indium suffers of a low diffusion coefficient and leads to a very low electron mobility.

In fact transport properties in MZT and MCT of the same band gap appear very near but this statement has to be better settled after a measure of the main band structure parameters. Nevertheless we can assert already now that MZT have electrical properties at least as suitables as the MCT ones for device elaboration, a definite advantage rising in its better stability.

References

[1] SHER A., CHEN A. B., SPICER A. E. and SHIH C. K., *J. Vac. Sci. Technol. A***3** (1985) 105.

[2] SHER A., BERDING M. A., CHEN A. B. and PATRICK R. S., *NATO Workshop,* Liège, 1988, to be published.

[3] TRIBOULET R., LASBLEY A., TOULOUSE B. and GRANGER R., *J. Cryst. Growth* **79** (1986) 695.

[4] TRIBOULET R., *J. Cryst. Growth* **86** (1988) 79.

[5] GRANGER R., LASBLEY A., ROLLAND S., PELLETIER C. M. and TRIBOULET R., *J. Cryst. Growth* **86** (1988) 682.

[6] TOULOUSE B., GRANGER R., ROLLAND S. and TRIBOULET R., *J. Phys. France* **48** (1987) 247.

[7] TRIBOULET R., LE FLOCH T. and SAULNIER J., *Proc. Conf. SPIE* (Insbruck) Ed. J. Besson (1986) p. 150.

[8] AMEURLAINE J., ROUSSEAU A., NGUYEN-DUY T. N. and TRIBOULET R., *Proc. SPIE ORLANDO* (Floride) 1988, Unpublished.

[9] TRIBOULET R., NGUYEN-DUY T. N. and DURAND A., *J. Vac. Sci. Technol. A* **3** (1985) 95.

[10] SMITH A., *Semiconductors* (Cambridge University Press) 1978, Chap. 5, p. 114.

[11] Measurements made at the West Microprobe Facility IFREMER, Brest. The x reported values are ten measurement averages.

[12] VYDYANATH H. R., *J. Electrochem. Soc* **128** (1981) 2609.

[13] HARMAN J. C., *J. Vac. Sci. Technol.* **5** (1987) 3055.

[14] TREGILGASS J., BECK J. and GNADE B., *J. Vac. Sci. Technol. A* **3** (1985) 150.

[15] MICKLETHWAITE W. F. H., *J. Appl. Phys.* **63** (1988) 2382.

[16] PETRITZ R. L., *Phys. Rev.* **110** (1958) 1254.

[17] DESTEFANIS G. L., *J. Vac. Sci. Technol. A* **3** (1985) 171.

[18] VYDYANATH H. R., *J. Electrochemi. Soc.* **128** (1981) 2619.

[19] RODE D. L., *Semiconductors and Semimetals,* Ed. R. K. Willarson and A. C. Beer (Academic Press, New York) 1975, Chap. I.

[20] LASBLEY A., GRANGER R., PELLETIER C. M. and ROLLAND S., *J. Phys. France* **46** (1985) 1185.

[21] MROZKOWSKI J. A. and NELSON D. A., *J. Appl. Phys.* **54** (1983) 2041.

[22] WEILER M. H., *Semiconductors and Semimetals,* Ed. R. K. Willarson and A. C. Beer (Academic Press, New York) 1981, Vol. 16, p. 181.

[23] ZAWADSKI W. and SZYMANSKA W., *Phys. Status Solidi* (B) **45** (1971) 415.

[24] IVANOV-OMSKII V. I., KOLOMIETS B. T., MALKOVA A. A. and MEKHTIEV A. S., *Phys. Status Solidi* **32** (1909) K84.

[25] LAWAETZ P., *Phys. Rev. B* **4** (1971) 3460.

[26] JEDRZEJCZAK A. and DIETL T., *Phys. Status Solidi* (B) **76** (1976) 737.

[27] CARDONA M., *J. Phys. Chem. Solids* **24** (1963) 1543.

[28] STRADLING R. A., *Solid State Commun.* **6** (1968) 665.

[29] FINKMAN E., *J. Appl. Phys.* **54** (1983) 1883.

[30] SCHMIT J. L., *J. Appl. Phys.* **41** (1970) 2876.